Supporting Information

An innovative and efficient preparation of mesocarbon microbeads by the delayed capillary breakup method and their electrochemical performance

DONG Si-Lin [1], YANG Jian-Xiao [1*], CHANG Sheng-Kai [1], SHI Kui [1], LIU Yue [1], ZOU Jia-Ling [1], LI Jun [2]

(1. Hunan Province Key Laboratory for Advanced Carbon Materials and Applied Technology, College of Materials Science and Engineering, Hunan University, Changsha, 410082, CHINA;
2. School of Chemistry and Biological Engineering, Changsha University of Science and Technology, Changsha, 410114, CHINA)

Corresponding author:

YANG Jian-xiao, E-mail: yangjianxiao@hnu.edu.cn

Author introduction:

DONG Si-lin, E-mail: silindong@hnu.edu.cn

Experimental

The corresponding characteristic parameters of samples were collected and calculated from the TG-DSC, FTIR, Raman, porosity parameters, XRD and GCD analysis as follow:

In the TG-DSC analysis, T_d (decomposition temperature) and W (coking values at 1000 °C) were collected from the TG curves of samples in the nitrogen atmosphere. T_i (initial decomposition temperature), T_f (final decomposition temperature), $\triangle T$ (difference between T_i and T_f), $\triangle H$ (enthalpy change) and $\triangle H/\triangle T$ (enthalpy difference per temperature) were collected and calculated from the DSC curves of samples in the air atmosphere.

In the FTIR analysis, the orthosubstitution index (I_{OS}), C–H substitution index (I_{CHS}) and the alkyl index (I_A) were calculated according to the relevant literature. I_{OS} is the proportion of aromatic rings with ortho substituents (i.e., four neighboring hydrogen atoms) compared with the proportion with all aromatic rings at least one hydrogen atom and represents the condensation degree. I_{CHS} gives the proportion of aromatic carbon atoms attached to $–CH_3$ or $–CH_2$ groups. I_A represented the fraction of alkyl groups that were linked to nonaromatic carbon atoms (instead of aromatic carbon atoms). The specific calculation formula were shown in equation (1-3).

$$I_{OS} = \frac{\mathrm{Abs}_{750}}{\mathrm{Abs}_{750}+\mathrm{Abs}_{814}+\mathrm{Abs}_{840}+\mathrm{Abs}_{880}} \quad (1)$$

$$I_{CHS} = \frac{\mathrm{Abs}_{2920}}{\mathrm{Abs}_{3050}+\mathrm{Abs}_{2920}} \quad (2)$$

$$I_A = \frac{\mathrm{Abs}_{2960}}{\mathrm{Abs}_{3050}+\mathrm{Abs}_{2960}} \quad (3)$$

In the Raman analysis, D peak near 1300 cm^{-1}, corresponding to graphite structure with defects or disorder; G peak near 1580 cm^{-1}, corresponding to good graphite structure. In addition, the ungraphitized samples have a broadened A peak between 1500 and 1550 cm^{-1}, which is related to the amorphous carbon structure, while the graphitized samples have a D' peak near 1620 cm^{-1}, which is mainly derived from a small amount of disordered graphite structure that has not been transformed into ordered graphite after graphitization. D' peak weakens or even disappears with the increase of graphitization. The peak ratio of D and G peaks (I_D/I_G) is commonly used to evaluate the graphitization degree of carbon materials, and the peak ratio of A and G peaks (I_A/I_G) or the peak ratio of D' and G peaks ($I_{D'}/I_G$) reflects the disorder degree of carbon materials.

In the porosity parameters analysis, the BET specific surface area (S_{BET}) and average pore diameter (D) were calculated by using the Brunauer–Emmett–Teller (BET) equation. The pore size distributions were acquired by applying the DFT method. The *t*-plot method was applied to evaluate the micropore volume (V_{mic}). The total pore volume (V_{tot}) was evaluated at a relative pressure of 0.99, and the mesopore volume (V_{mes}) was calculated by subtracting V_{mic} from V_{tot}.

In the XRD analysis, λ (incident X-ray wavelength), θ (Bragg diffraction Angle), d_{002} (the layer spacing), β (half the width of the diffraction peak), L_c (the stacking thickness of carbon microcrystals), L_a (the crystal plane size of carbon microcrystals), N (number of carbon layer stacking in graphite microcrystalline), 0.3440 (layer spacing of completely ungraphitized carbon crystals), 0.3354 (layer spacing of ideal graphite crystal) and G (degree of graphitization) were collected and calculated from the XRD spectras of samples. The specific calculation formula were shown in equation (4-8).

$$d_{002} = \frac{\lambda}{2sin\,\theta_{002}} \quad (4)$$

$$L_C = \frac{0.89\lambda}{\beta_{002}\,cos\,\theta_{002}} \quad (5)$$

$$L_a = \frac{1.84\lambda}{\beta_{110}\,cos\,\theta_{110}} \quad (6)$$

$$N = \frac{L_C}{d_{002}} + 1 \quad (7)$$

$$G = \frac{0.3440 - d_{002}}{0.3440 - 0.3354} \times 100\% \quad (8)$$

In the GCD analysis, I (discharging current), $\triangle t$ (discharging time), m (the mass of the active substance) and $\triangle V$ (discharging voltage) were collected and calculated from the GCD curves of samples. The calculation formula used in the three-electrode system for mass specific capacitance was shown in equation (9).

$$C = \frac{I\triangle t}{m\triangle V} \quad (9)$$

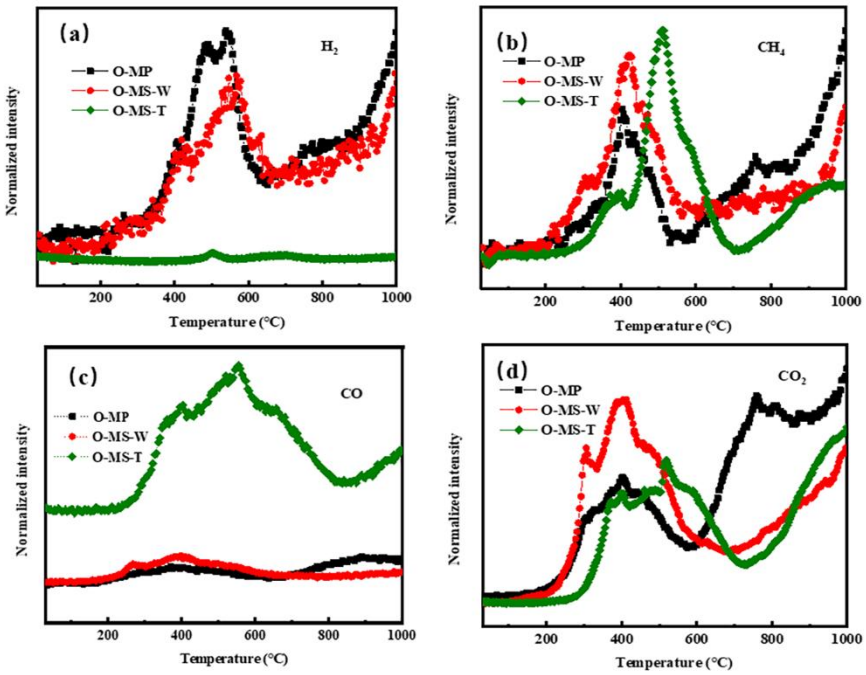

Fig. S1 TG-MS curves of O-MP, O-MS-W and O-MS-T in nitrogen atmosphere (a) H_2, (b) CH_4, (c) CO, (d) CO_2.

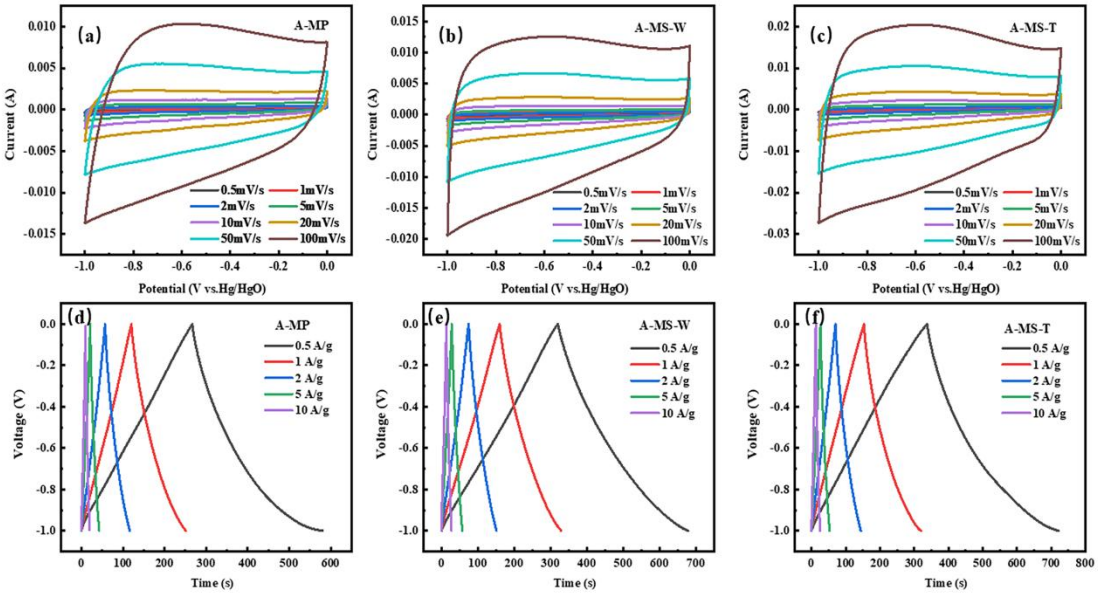

Fig. S2 CV curves at the scanning speed of 0.5, 1, 2, 5, 10, 20, 50, 100 mV s^{-1} of (a) A-MP, (b) A-MS-W, (c) A-MS-T and GCD curves at the current density of 0.5, 1, 2, 5, 10 A g^{-1} of (d) A-MP, (e) A-MS-W, (f) A-MS-T.

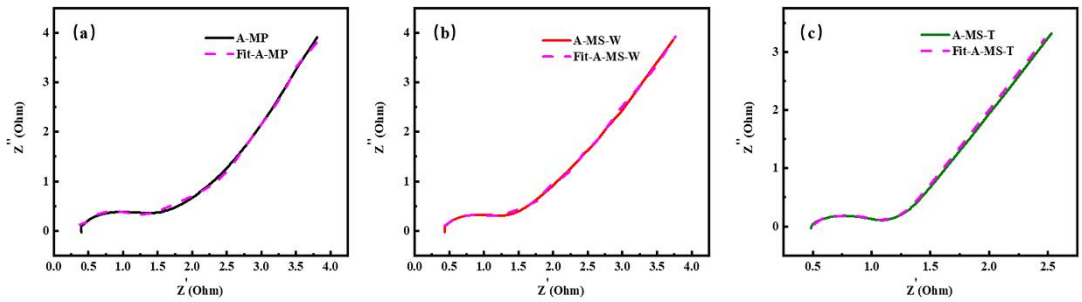

Fig. S3 The fitted EIS curves of (a) A-MP, (b) A-MS-W and (c) A-MS-T.

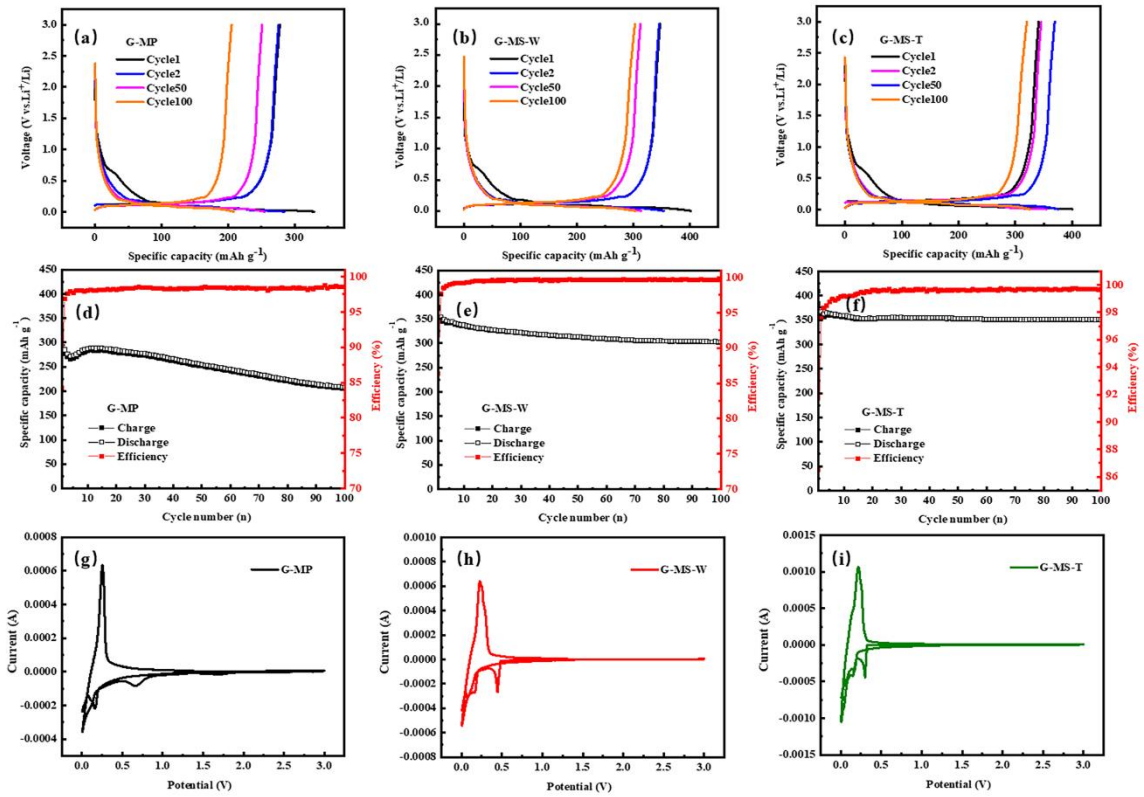

Fig. S4 The 1st, 2nd, 50th, and 100th discharge/charge curves of (a) G-MP, (b) G-MS-W, (c) G-MS-T between 0.005 and 3.0 V at a current density of 100 mA g^{-1}, cycling performance and coulombic efficiency at 100 mA g^{-1} of (d) G-MP, (e) G-MS-W, (f) G-MS-T and CV plots of (g) G-MP, (h) G-MS-W, (i) G-MS-T in the first cycle between 0.005 and 3.0 V at a scan rate of 0.1 mV s^{-1}.

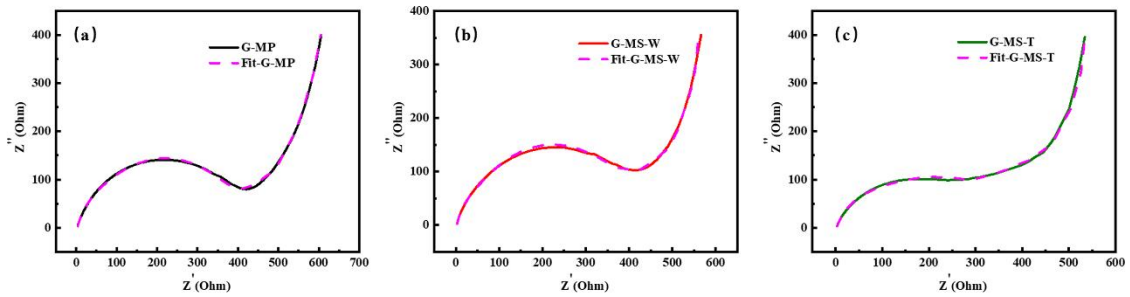

Fig. S5 The fitted EIS curves of (a) G-MP, (b) G-MS-W and (c) G-MS-T.

Table S1 Rate capacity of G-MP, G-MS-W and G-MS-T.

Samples	Specific capacity (mAh g-1)					
	0.05 A g^{-1}	0.1 A g^{-1}	0.5 A g^{-1}	1 A g^{-1}	2 A g^{-1}	0.05 A g^{-1}
G-MP	411.1	276.7	91.5	34.6	20.1	250.7
G-MS-W	403.8	298.0	155.1	92.7	52.5	297.1
G-MS-T	462.8	339.7	194.3	90.2	53.0	344.6